Bedford Institute of Oceanography
l'institut oceanographiqué de Bedford
Dartmouth/Nova Scotia/Canada

Tides of Hudson Strait

A. K. Easton

Report Series/BI-R-72-6/June 1972

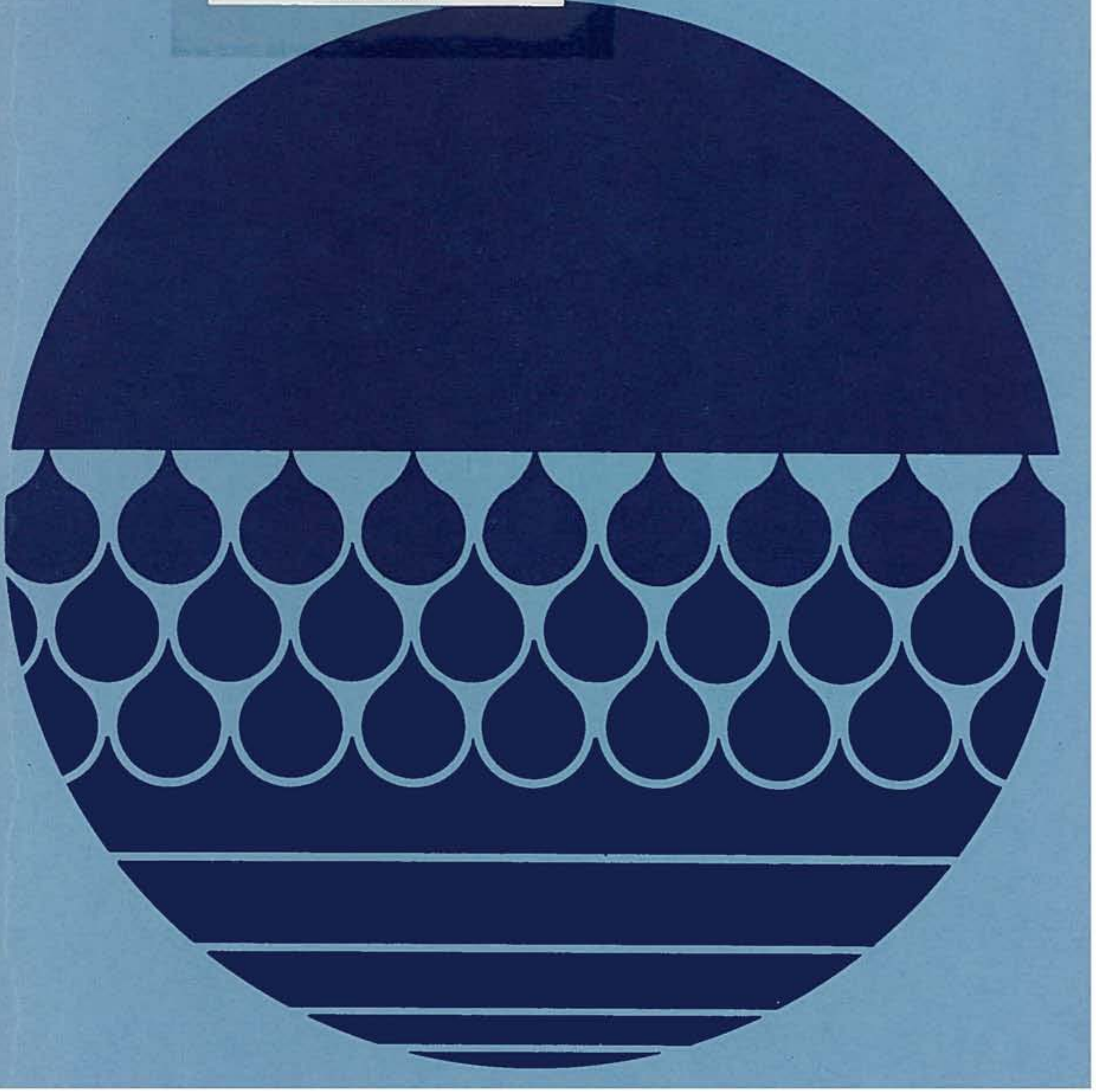

Cover Design/Keith Clarridge

BEDFORD INSTITUTE OF OCEANOGRAPHY

Dartmouth, Nova Scotia
Canada

TIDES OF HUDSON STRAIT

by
A.K. Easton

Atlantic Oceanographic Laboratory
Marine Sciences Branch
Department of the Environment

This is an internal technical report which has received only limited circulation. On citing this report the reference should be followed by the words 'UNPUBLISHED MANUSCRIPT'.

JUNE 1972 REPORT SERIES BI-R-72-6

ABSTRACT

A numerical model has been used to compute the characteristics of the M_2 tidal constituent in Hudson Strait. The surface elevation is compared with observations in the form of co-tidal and co-amplitude charts while the tidal streams are compared with data from the central part of the strait.

INTRODUCTION

Although tide measurements had been made at selected stations in Hudson Strait (Fig. 1) ever since the Gordon Expeditions of 1884-1886, it was only in the 1950's that the tides in Ungava Bay, with ranges of 13.7 metres at Koksoak River entrance and 16.6 metres in Leaf Basin, were recorded (Dunbar, 1958). Recently, Collin (1966) has called these the largest tides in the world. To date, records have been analyzed for 23 ports (Table 1).

The tides of Hudson Strait are strictly semidiurnal, e.g. at Diana Bay, the standard port for purposes of tide predictions, the amplitude ratio $M_2:S_2:N_2:K_1:O_1$ is 100:34:20:5:3. Hence, the tides are well represented by the spring pattern (Dohler, 1964). The mean spring range increases from 6 metres at the Atlantic Ocean to over 9 metres near Big Island and then decreases to less than 5 metres and 3 metres at the north and south shores, respectively, of the Hudson Bay entrance. At the head of Ungava Bay, the mean spring range is in excess of 10 metres. The phase of the tide increases westwards.

In this paper we will confine our attention to the dominant M_2 constituent. A numerical model, in which the surface elevation is specified at the open boundaries, is employed to compute the surface elevation and horizontal transports throughout the Strait. The surface elevation is summarized in co-tidal and co-amplitude charts so that they may be compared with observed coastal values. The computed streams are presented as co-tidal and co-amplitude charts for the u and v velocity components. They are compared with observed data between Big and Wales Islands (Anonymous, 1960).

NUMERICAL MODEL

For the purposes of this investigation, we will use the shallow water equations of motion and continuity without any external forces. If we neglect the non-linear convection terms and integrate the equations over the depth, they may be expressed in the form

$$\frac{\partial Z}{\partial t} = \frac{\partial M}{\partial x} + \frac{\partial N}{\partial y}, \qquad (1)$$

$$\frac{\partial M}{\partial t} = fN - gH\frac{\partial Z}{\partial x} - GM, \qquad (2)$$

$$\frac{\partial N}{\partial t} = - fM - gH\frac{\partial Z}{\partial y} - GN, \qquad (3)$$

where the x and y axes are in the easterly and northerly directions, respectively, $Z(x,y,t)$ is the surface elevation above sea level, $M(x,y,t)$ and $N(x,y,t)$ are the x- and y-components of the volume transport, f is the Coriolis parameter, g is the gravitational acceleration, $H(x,y,t)$ is the total depth and

$$G(x,y,t) = \frac{r\,(M^2 + N^2)^{\frac{1}{2}}}{H^2},$$

where r is the coefficient of quadratic friction. This form of the friction term is the most appropriate one when the velocity is independent of depth and the current data for the central section of the Strait (Anonymous, 1960) indicates that this is true.

Following Miyazaki (1965), Reid and Bodine (1968) and others, we approximate all differentials by centre differences, in which i, j and n represent the coordinates x, y and t, respectively. From equation (1), we obtain directly

$$Z_{i,j}^{\;n} = Z_{i,j}^{\;n-2} - \frac{\tau}{\ell}\,[M_{i+1,j}^{\;n-1} - M_{i-1,j}^{\;n-1} + N_{i,j+1}^{\;n-1} - N_{i,j-1}^{\;n-1}], \qquad (4)$$

where τ is the time step and ℓ is the grid interval in both the x and y directions. In order that we may compute elevations for even values of n and (i+j) as is suggested by (4), we require that the transports be calculated for the odd values. Thus, those values of M and N appearing on the right-hand side of equations (2) and (3), which are required for even n, are replaced by the average of the values for times n-1 and n+1. This procedure is suggested by both Miyazaki (1965) and Fisher (1965) as a means of avoiding computational instability. The modulus of the transport incorporated in G is calculated from values at time n-1. Although this procedure results in an apparently implicit numerical scheme, the equations may be solved to yield the explicit forms

$$\begin{aligned}
[(1+\beta)^2 + \alpha^2]M_{i+1,j}^{\;n+1} &= (1-\beta^2-\alpha^2)M_{i+1,j}^{\;n-1} + 2\alpha N_{i+1,j}^{\;n-1} \\
&\quad - \frac{g\tau}{\ell}\,H_{i+1,j}^{\;n}\,[(1+\beta)(Z_{i+2,j}^{\;n} - Z_{i,j}^{\;n}) \\
&\quad + \alpha\,(Z_{i+1,j+1}^{\;n} - Z_{i+1,j-1}^{\;n})] \qquad (5)
\end{aligned}$$

$$\begin{aligned}
[(1+\beta)^2 + \alpha^2]N_{i+1,j}^{\;n+1} &= -2\alpha M_{i+1,j}^{\;n-1} + (1-\beta^2-\alpha^2)N_{i+1,j}^{\;n-1} \\
&\quad + \frac{g\tau}{\ell}\,H_{i+1,j}^{\;n}\,[\alpha(Z_{i+2,j}^{\;n} - Z_{i,j}^{\;n}) \\
&\quad - (1+\beta)(Z_{i+1,j+1}^{\;n} - Z_{i+1,j-1}^{\;n})] \qquad (6)
\end{aligned}$$

where

$$\beta = \frac{\tau r[(M_{i+1,j}^{\;n-1})^2 + (N_{i+1,j}^{\;n-1})\,]^{\frac{1}{2}}}{(H_{i+1,j}^{\;n})^2},$$

$$\alpha = \tau f,$$

$$H_{i+1,j}^{\;n} = D_{i+1,j} + \frac{1}{4}\,(Z_{i+2,j}^{\;n} + Z_{i,j}^{\;n} + Z_{i+1,j+1}^{\;n} + Z_{i+1,j-1}^{\;n})$$

and D is the depth below mean sea level. Along the boundaries where equations (4), (5) and (6) do not apply, the space derivatives in (1), (2) and (3) are replaced by either forward or backward differences.

A square grid with $\ell = 10.5$ km has been constructed on the basis of the Canadian Hydrographic Service Chart No. 5450, which presents Hudson Strait in Mercator projection. The coastline has been approximated by straight line segments parallel to either the x axis, on which N=0, or parallel to the y axis, on which M=0 (Fig. 2). Z is calculated at all corner points. Along the open boundaries, the tide elevation is specified in the form

$$Z_{ij}^{\;n} = A_{ij}\,\cos\left(\frac{2\pi n}{T} - g_{ij}\right), \qquad (7)$$

where A_{ij} is the amplitude and g_{ij} is the phase of the M_2 tide which has a period T = 12.42 hours. Values of A and g have been interpolated by means of a vectorial weighting of the values at Port Burwell and Acadia Cove for the eastern entrance and of the values at Digges Harbour, Port de Boucherville and Schooner Harbour at the western entrance.

Initial conditions were set as follows. At t=0 (n=0), all Z_{ij} were set equal to zero except those at the open boundaries which are given by (7). At $t=\tau$ (n=1), all M_{ij} and N_{ij} were set equal to zero. Then (4), (5) and (6) were used in turn to calculate Z for even time steps and M and N for odd time steps.

The above numerical scheme is stable provided that the time step

$$\tau < \frac{\ell}{\sqrt{2g\ H_m}},$$

where H_m is the maximum value of H. τ was selected as 75 seconds. In spite of this condition, spurious waves are still generated in the subsequent calculations. The waves with small wavelengths have been filtered by means of the space average

$$\bar{X}_{ij}{}^{n} = \frac{1}{8}\,[4\,X_{ij}{}^{n} + X_{i+1,j+1}{}^{n} + X_{i+1,j-1}{}^{n} + X_{i-1,j+1}{}^{n} + X_{i-1,j-1}{}^{n}],$$

where X represents Z, M and N. This was only used at the interior points. Other waves corresponding to the normal modes of the Strait were also initiated. These decayed due to the inherent stability of the computational scheme.

After four tidal cycles, values of successive maxima and minima of the surface elevation differed by less than 2 cm for all grid points and the corresponding phase differences were within 2° of 180°. This is evidence that the non-linear friction effect is small as well as that the effect of initial conditions is then negligible. The discharges also followed the almost pure sinusoidal motion. The average values for the extrema during the fifth tidal cycle were taken to be the amplitudes and phases of Z, M and N. The surface elevation has been summarized as co-tidal and co-range charts (Fig. 3). The discharges M and N have been scaled to yield u and v, the x^- and y^- components of the velocity

$$u = M/D,$$

$$v = N/D.$$

These velocities are also summarized in co-tidal and co-amplitude charts (Fig. 4, 5).

DISCUSSION

First of all, we will compare the surface tidal pattern suggested by the coastal observations (Fig. 1) with that predicted by the model (Fig. 3), remembering that the phase and amplitude gradients at the open boundaries, including between Digges and Schooner Harbours, are imposed by the boundary conditions. It is evident that the general features are predicted well but the accuracy at particular ports is often poor.

The model correctly predicts that the tide progresses from the Atlantic Ocean toward Hudson Bay, that the amplitudes on the north shore of the Strait are much larger than on the south and that there are larger amplitudes near Lake Harbour than at either boundary. It also shows a trough of low amplitudes extending across the mouth of Ungava Bay and considerable amplification toward the head of the Bay.

A closer inspection of the predicted values show that there are marked differences with the observed pattern. Amplitudes are low (they are 3 metres instead of 4 metres at Koksoak River) and phases are large (there is a phase difference of 42° instead of 15° between Port Burwell and Diana Bay) (Table 2). On the other hand, phase differences between ports away from the boundaries agree closely with observations, e.g. the phase difference between Koksoak River and Diana Bay should be 5° and is 8°. Thus, we should look more carefully at the values near the boundaries including the predicted amphidromy.

The amphidromic point near Port Burwell is a very interesting outcome of the model. Even if it is caused entirely by the boundary conditions, it suggests that the boundary conditions which must be imposed here are critical. Its intensity and position would greatly influence the amplitudes and phases in the Strait. Data available for the Labrador Coast indicate that the tidal range decreases sixfold in a distance of 200 km from the Hudson Strait entrance and thus emphasizes the special nature of the area near Port Burwell. Thus, there is evidence to support at least a degenerate amphidromy although present data suggests it probably is just outside the strait. Another possible source of error is the neglect of Gabriel Strait. But since its cross-sectional area is only 14% of that of the main channel, this seems a good approximation. At the western entrance, Digges Harbour constants seem to be a poor representation of the tides of that area and probably values from Port de Laperriere would be better even though they are only based on 15 days data.

The strengths of the tidal streams (Fig. 4, 5) at the ends of the Strait are related to the boundary conditions imposed but certainly the maximum currents are experienced here. At the eastern entrance the computed transport is $40\text{x}10^7\ m^3$/sec. In the interior, the velocity contours reflect the influence of bottom topography. Thus there are velocities of only 30 cm/sec in the deep channel inside the Atlantic entrance and velocities greater than 100 cm/sec in the shallower areas at the entrance to Ungava Bay and in the western end of the Strait. The v velocity component is, as expected, stronger than the u component at the head of Ungava Bay but elsewhere it is weaker.

Since u and v are in phase in Ungava Bay, the current direction does not rotate. At the entrance to Ungava Bay, the current rotates in a clockwise direction. In the central Strait region, u and v are out of phase so that the current direction is entirely along the channel. The average amplitude of the volume transport at the Wales Island-Big Island section is 1.0×10^7 m^3/sec compared with 1.2×10^7 m^3/sec determined from Farquharson's measurements (Anonymous, 1960). The computed phase of 85° differs from the observed 111°; the phase of the surface elevation at Diana Bay differs from its observed value by 29°. The good agreement for the discharges is a consequence of the very small change in the discharge along this uniform channel.

Another interesting feature of the tides in this central region is that they are purely progressive and the high tides and maximum inward currents occur simultaneously. To the west, the current precedes the high tide while to the east, the current lags it. At the head of Ungava Bay the tides approach a standing character.

CONCLUSIONS AND RECOMMENDATIONS

This numerical model, which is basically a modification of that used by Miyazaki (1965), has proved very successful. A particular advantage is that the values of Z, M and N are calculated on the solid boundaries where the water depth must always be greater than the tide range. At present, the model does not include the convection terms.

Results of this model differ somewhat from observations in terms of actual numbers but the general features are reproduced. In particular, the strong Coriolis effect is more evident in the smaller amplitudes of the surface elevation on the south shore of the strait than on the north shore. The smaller amplitudes are also found across the north of Ungava Bay. Further, amplitudes are larger in the centre of the Strait than at either end.

Perhaps the calculated streams are the greatest achievement of this model since they form the first complete set of values for the Strait. The relatively small streams in the central section of the Strait agree satisfactorily with Farquharson's measurements (Anonymous, 1960). At the Atlantic entrance, where the strength is determined by the boundary conditions, maximum currents of over 300 cm/sec are predicted. It is also very interesting to be able to see the change in the character of the tide between the extremes of being totally progressive in the central Strait region and of being standing at the head of Ungava Bay.

The aim of future studies of the tides of Hudson Strait will be to obtain more accurate predictions. Since this requires more accurate boundary values, a field survey should be undertaken to measure tidal heights and currents at the boundary grid points. With these values, the study will probably resolve the mystery of the amphidromic point near Port Burwell. However, progress in this direction could be attempted with shore-based recorders, particularly along the eastern shore of Ungava Bay where the tides have not been measured to date. This will also fix the co-tidal and co-amplitude lines for Ungava Bay. The need for boundary conditions at the western end of the Strait could be avoided by a larger model consisting of the entire Hudson Bay, Hudson Strait, Foxe Basin system but I think this advantage would be outweighed by the increased computing effort and perhaps a larger grid length with the loss of local accuracy.

ACKNOWLEDGEMENT

This research was begun while the author was located in Ottawa at the Division of Oceanographic Research. Throughout, the author has held a Postdoctorate Fellowship of the National Research Council of Canada. The tidal data was supplied by Mr. G. Dohler, Tides and Water Levels, Ottawa.

REFERENCES

ANONYMOUS. 1960. Tidal and Oceanographic Survey Hudson Strait August and September, 1959. Data Record, Canadian Hydr. Serv., Dept. Mines and Tech. Surveys.

COLLIN, A.E. 1966. Hudson Bay and Approaches. Encyclopedia of Oceanography, Ed. R.W. Fairbridge. Reinhold Pub. Co., N.Y.

DOHLER, G. 1964. Tides in Canadian Waters, Canadian Hydr. Serv., Mar. Sci. Branch, Dept. Mines and Technical Surveys.

DUNBAR, M.J. 1958. Physical Oceanographic Results of the 'Calanus' Expeditions in Ungava Bay, Frobisher Bay, Cumberland Sound, Hudson Strait and Northern Hudson Bay, 1949-1955. *J. Fish. Res. Bd. Canada,* 15, 155-201.

FISHER, G. 1965. Comments on 'Some problems involved in the numerical solution of Tidal Hydraulics Equations'. Mon. Weath. Rev., 93, 110-111.

MIYAZAKI, M. 1965. A numerical calculation of the storm surge of Hurricane Carla in the Gulf of Mexico. *Oceanogr. Mag.,* 17, 109-140.

REID, R.O., and B.R. BODINE. 1968. Numerical model for storm surges in Galveston Bay. *J. Waterways and Harbors Div.,* Proc. A.S.C.E., 94, 33-57.

TABLE 1

Tidal constants for Hudson Strait ports (time zone + 4 hr). Amplitudes H are cm, phases g are degrees, L represents the length in days of data analyzed.

		M_2		S_2		N_2		K_1		O_1	
Port	L	H	g	H	g	H	g	H	g	H	g
Acadia Cove	15	216	240	89	276	43	-	13	130	15	97
Lake Harbour	15	360	255	131	314	69	222	13	115	4	63
Ashe Inlet	29	335	259	121	317	67	237	16	118	6	4
Schooner Harbour	29	208	345	71	39	42	318	8	162	6	145
Port Burwell	29	214	238	65	288	42	206	13	105	9	58
Koksoak River	29	409	258	136	312	76	224	16	106	13	67
Leaf Basin	29	433	280	137	344	92	281	19	128	7	99
Hopes Advance Bay	29,29	388	254	125	310	83	216	21	112	10	59
Agvik Island	29	349	254	117	305	65	227	18	125	11	41
Pikiyulik Island	29	305	280	95	322	55	252	15	120	6	79
Basking Island	29	317	282	100	343	58	263	14	127	12	77
Diana Bay	29,29	293	253	99	305	59	226	16	103	9	61
Stupart Bay	15	275	254	93	312	55	-	14	114	9	22
Doctor Island	15	258	266	88	319	52	339	15	133	8	91
Wakeham Bay	29	337	263	163	309	70	240	13	92	10	67
Douglas Harbour	29	259	260	92	328	48	243	11	75	4	8
Deception Bay	15	169	281	63	330	29	255	9	89	3	303
Sugluk	15,29	155	284	59	334	31	256	10	105	4	51
Digges Harbour	29	100	308	39	355	20	280	6	119	4	91
Port de Laperriere	15	94	297	38	352	18	-	4	81	1	148
Port de Boucherville	29	145	299	54	356	27	-	7	128	8	39

TABLE 2

Computed surface elevation constants of M_2 for selected ports. Amplitudes H are cm, phases g are degrees (time zone + 4 hr).

Port	H	g
Lake Harbour	289	279
Koksoak River	293	290
Hopes Advance Bay	277	279
Diana Bay	242	282
Doctor Island	251	286
Sugluk	179	307

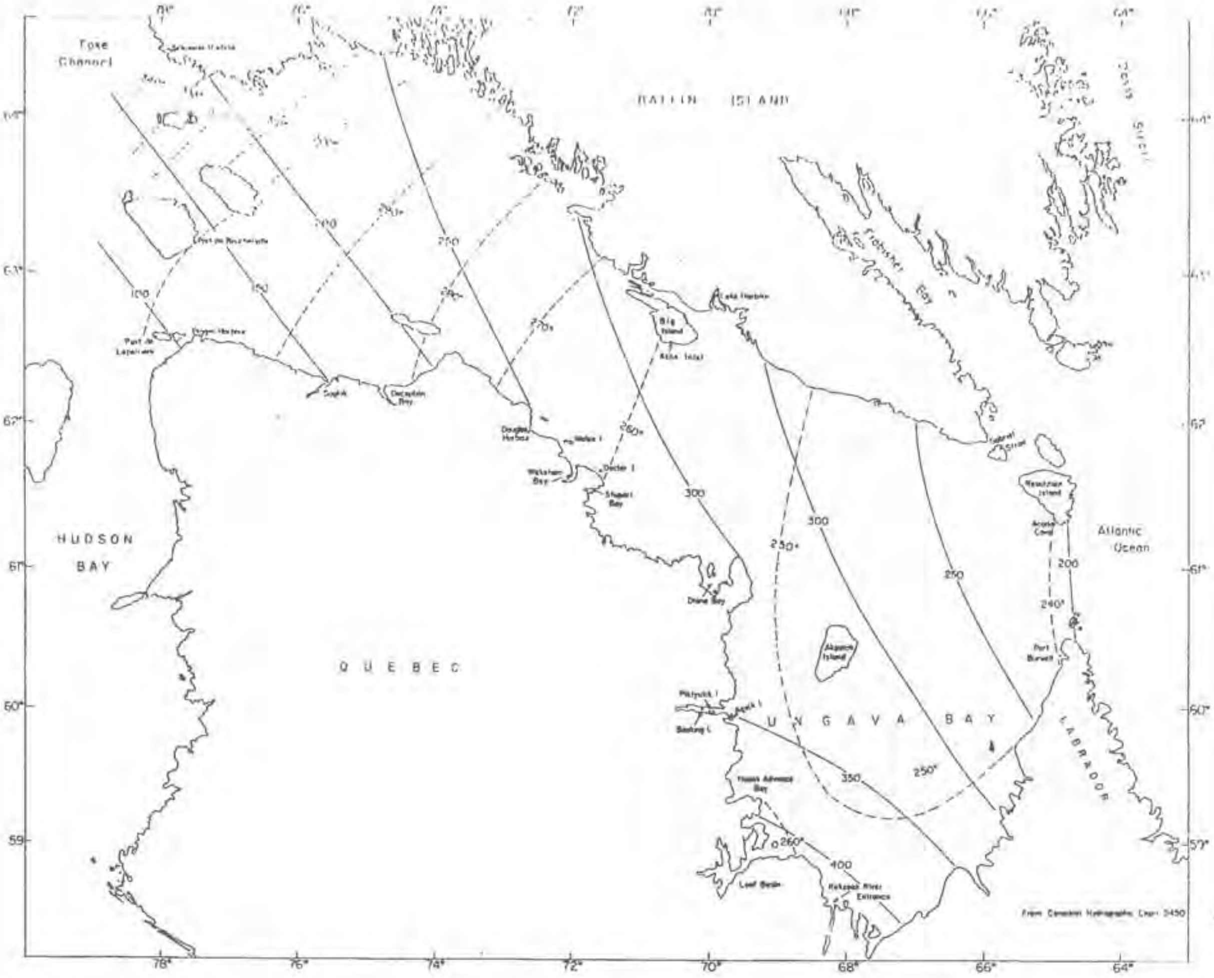

FIGURE 1: Tidal stations in Hudson Strait and the inferred M_2 co-tidal and co-amplitude charts of the surface elevation. Phases are g^o (time zone + 4 hr); amplitudes are cm.

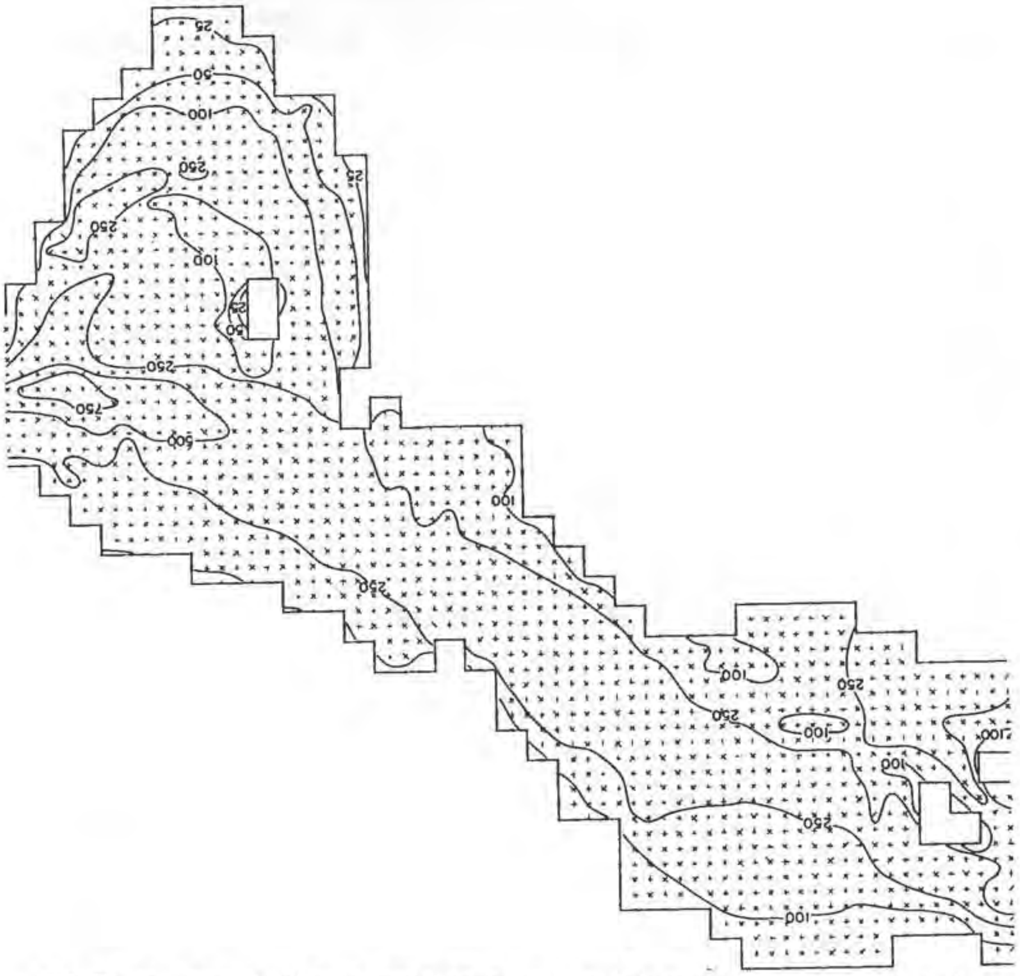

FIGURE 2: Hudson Strait grid of Z points (+) and M and N points (x) and the contours in m of the depth D. The grid interval is 10.5 km.

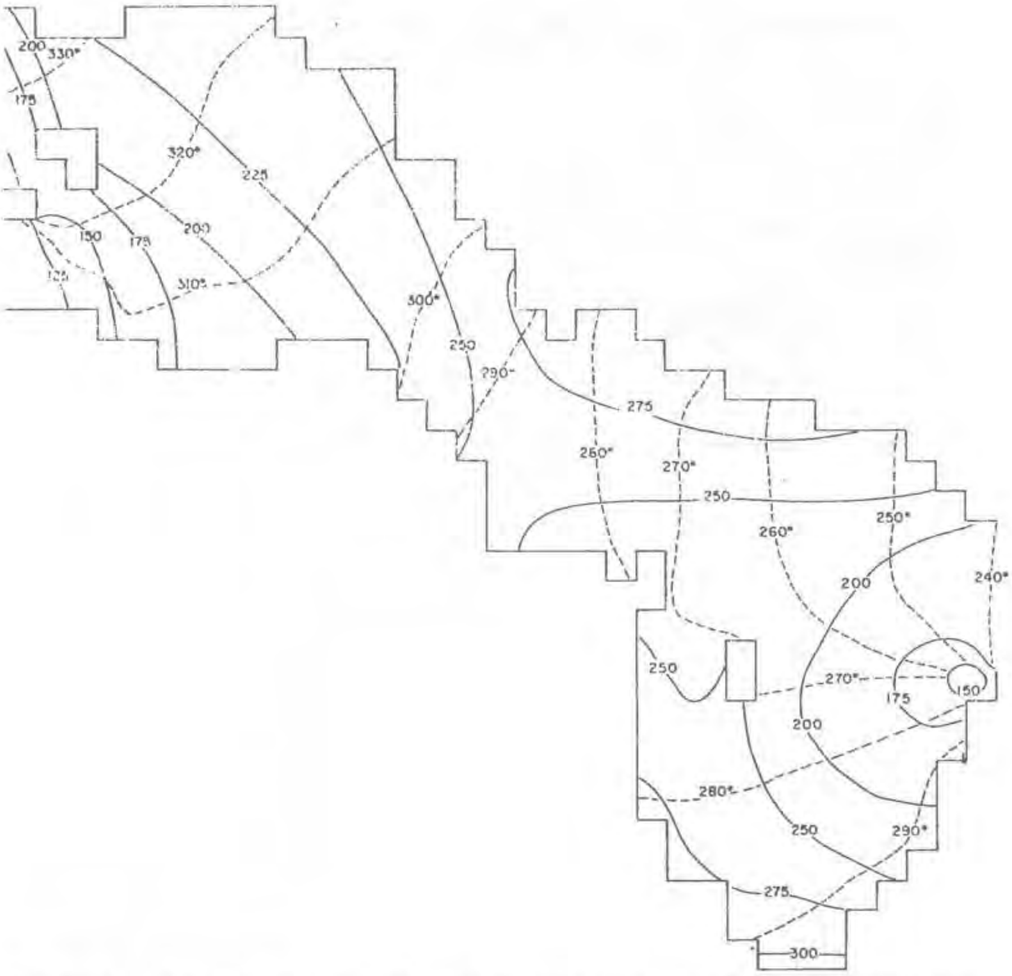

FIGURE 3: Computed M_2 co-tidal and co-amplitude charts of the surface elevation for Hudson Strait. Phases are g° (time zone + 4 hr); amplitudes are cm.

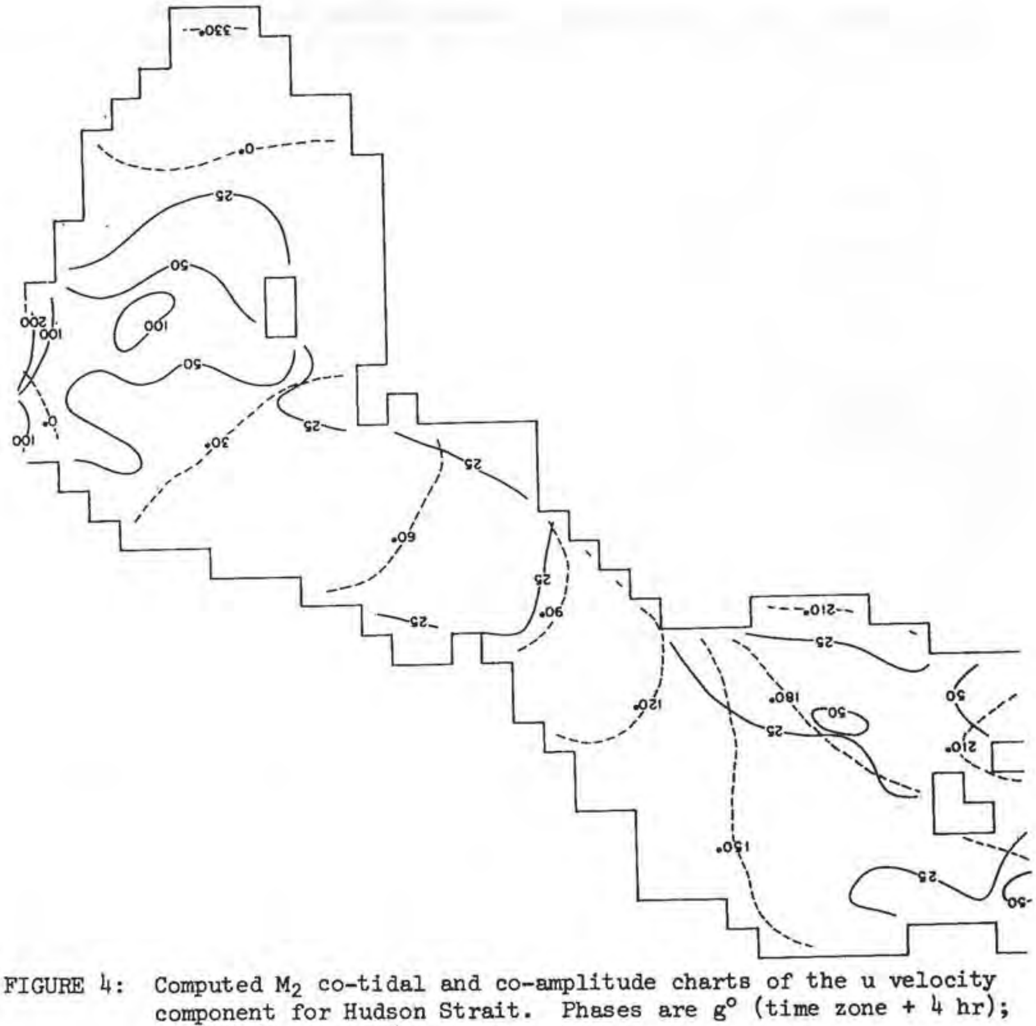

FIGURE 4: Computed M_2 co-tidal and co-amplitude charts of the u velocity component for Hudson Strait. Phases are g° (time zone + 4 hr); amplitudes are cm/sec.

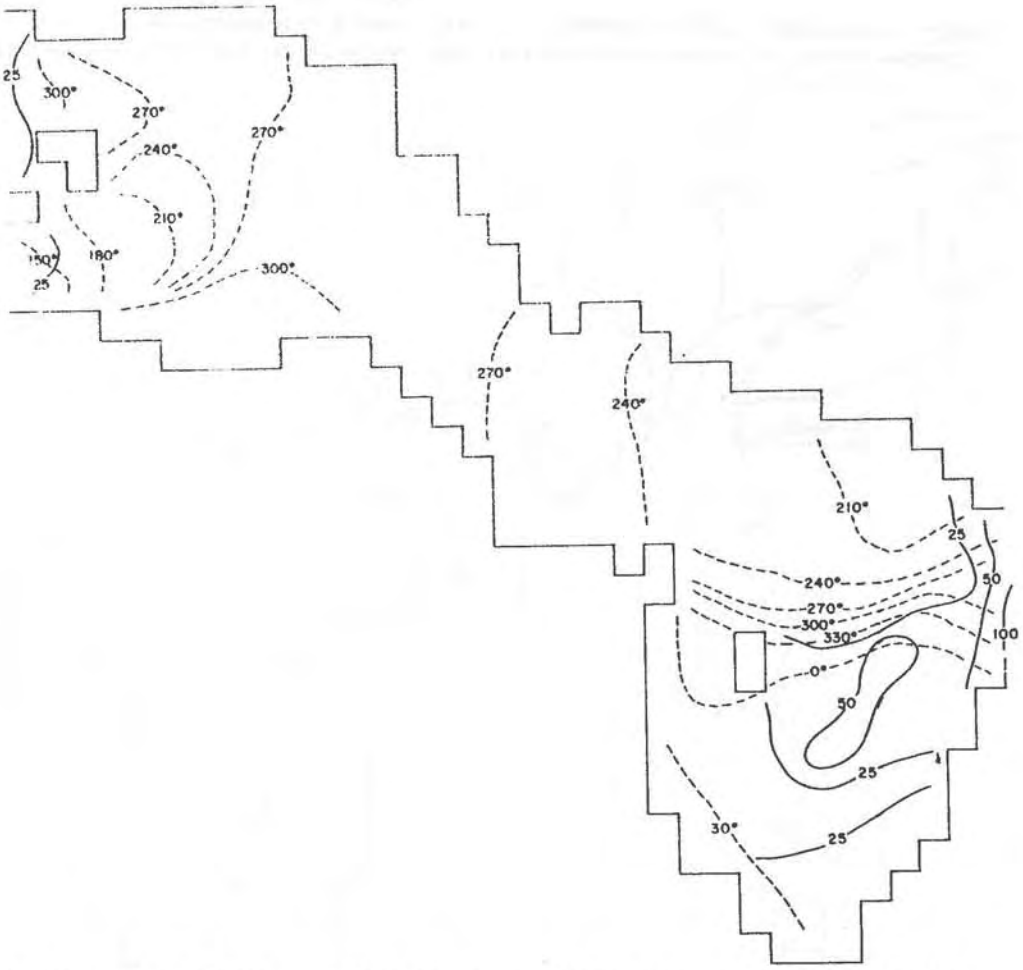

FIGURE 5: Computed M_2 co-tidal and co-amplitude charts of the v velocity component for Hudson Strait. Phases are g° (time zone + 4 hr); amplitudes are cm/sec.